The Journal of Experimental Biology 203,3319–3332 (2000)
Printed in Great Britain © The Company of Biologists Limited 2000
JEB2895

EFFECTS OF BODY SIZE ON TAKE-OFF FLIGHT PERFORMANCE IN THE PHASIANIDAE (AVES)

BRET W. TOBALSKE* AND KENNETH P. DIAL

Division of Biological Sciences, University of Montana, Missoula, MT 59812, USA and *Concord Field Station, Museum of Comparative Zoology, Harvard University, Old Causeway Road, Bedford, MA 01730, USA*

*Present address: Department of Biology, University of Portland, 5000 North Willamette Boulevard, Portland, OR 97203, USA (e-mail: tobalske@up.edu)

Accepted 3 August; published on WWW 9 October 2000

Summary

To evaluate the mechanisms responsible for relationships between body mass and maximum take-off performance in birds, we studied four species in the Phasianidae: northern bobwhite (*Colinus virginianus*), chukar (*Alectoris chukar*), ring-necked pheasant (*Phasianus colchicus*) and wild turkey (*Meleagris gallopavo*). These species vary in body mass from 0.2 to 5.3 kg, and they use flight almost solely to escape predators. During take-off, all the species used a similar wingbeat style that appeared to be a vortex-ring gait with a tip reversal during the upstroke. The tip reversal is unusual for birds with rounded wings; it may offer an aerodynamic advantage during rapid acceleration. Flight anatomy generally scaled geometrically, except for average wing chord and wing area, which increased more than expected as body mass (*m*) increased. Pectoralis strain varied from 19.1 to 35.2 % and scaled in proportion to $m^{0.23}$. This positive scaling is not consistent with the widely held assumption that muscle strain is independent of body mass among geometrically similar species. The anatomy of the species precluded measurements of *in vivo* pectoralis force using the strain-gauge technique that has been employed successfully in other bird species, so we could not directly test *in vivo* pectoralis force–velocity relationships. However, whole-body kinematics revealed that take-off power (P_{ta}), the excess power available for climbing and accelerating in flight, scaled in proportion to $m^{0.75}$ and that pectoralis mass-specific P_{ta} decreased in proportion to $m^{-0.26}$ and was directly proportional to wingbeat frequency. These trends suggest that mass-specific pectoralis work did not vary with body mass and that pectoralis stress and strain were inversely proportional, as expected from classical force–velocity models for skeletal muscle. Our observations of P_{ta} were consistent with evidence from other species engaged in escape flight and, therefore, appear to contradict evidence from studies of take-off or hovering with an added payload.

Key words: flight, scaling, muscle, pectoralis, strain, power, sonomicrometry, electromyography, Phasianidae.

Introduction

Casual field observation reveals that flight ability declines with increasing body size in birds and other flying animals, and it is generally expected that this trend will explain aspects of the ecology and evolution of flight. For example, within the Anseriformes, teal (*Anas* spp.) take off vertically while swans (*Cygnus* spp.) take off in a laboured manner, with a shallow initial angle of ascent. Since teal require less room than swans for take-off, teal may utilize smaller ponds with less open surface area. Some empirical data are consistent with these casual observations. Maximum acceleration during take-off or rates of vertical ascent are reported to decline with increasing body mass in small passerines (DeJong, 1983), aerial insectivores (Warrick, 1998) and doves and pigeons (Columbiformes; Seveyka, 1999). The percentage of time spent bounding in flap-bounding flight decreases with increasing body mass in woodpeckers (Picidae; Tobalske, 1996). What aspects of animal design can explain these trends?

One explanation for this is that the maximum mechanical power available from the flight muscles may be limited by wingbeat frequency (Pennycuick, 1975). In this line of reasoning, muscle strain (ε, the change in muscle length relative to resting length) and stress (σ, the force per unit cross-sectional area) are assumed to be independent of body mass. Mass-specific work, defined as $\varepsilon\times\sigma$/(density of muscle), is therefore assumed to be independent of mass, and mass-specific power is expected to scale in proportion to the frequency of cycles of limb movement. In birds, during maximal effort such as during take-off, wingbeat frequency is predicted to scale in proportion to $m^{-0.33}$, where *m* is body mass (Pennycuick, 1992), so the maximum mass-specific power available is expected to be proportional to $m^{-0.33}$. It is assumed that the mass-specific power required for flight at comparable velocities (i.e. not the same velocity) in birds or any flying objects of similar shape scales in proportion to $m^{0.16}$

(Pennycuick, 1975; Norberg, 1990). Ellington (1991) points out that changes in drag with changing Reynolds number across a wide range of body mass could result in mass-specific power required scaling in proportion to m^0. Thus, the mass-specific power required for flight is expected to scale between m^0 and $m^{0.16}$, resulting in a predicted adverse scaling of the power available relative to the power required that potentially accounts for a decline in flight ability as species become larger.

The only challenge to this explanation is provided by studies in which animals are maximally loaded with added weights. The maximum load that a flying animal can lift during take-off has been shown to be proportional to body mass over a broad range of body sizes (Marden, 1994) so that mass-specific lifting ability is independent of body size. Moreover, in hummingbirds (Trochilidae), maximum mass-specific lifting ability increases with increasing body mass (Chai and Millard, 1997). In these studies, direct measurements of mechanical power output were not obtained; rather, mechanical power costs were estimated using aerodynamic theory. From such estimates, it appears that the maximum mass-specific power available from the flight muscles scales positively with body mass ($m^{0.13}$), but less lift is produced per unit power output (Marden, 1994). For animals that are geometrically similar, Marden's (1994) multivariate regression indicates that lift per unit muscle power scales in proportion to $m^{-0.16}$; this offers an alternative explanation for a decline in flight ability with increasing body mass.

It nonetheless remains to be demonstrated directly that maximum mass-specific power available from the flight muscles can actually increase with increasing body mass. Assuming that wingbeat frequency scales as $m^{-0.33}$, muscle mass-specific work must be proportional to $m^{0.46}$ for mass-specific power to scale in proportion to $m^{0.13}$ (Ellington, 1991). This dramatic scaling relationship must involve an increase in ε, σ or both ε and σ. Chai and Millard (1997) report that wingbeat amplitude during maximal loading is greater in larger hummingbirds than in smaller hummingbirds. Presumably, wingbeat amplitude is proportional to ε; which provides some support for a positive scaling of maximum mass-specific work. At a given muscle contractile velocity, σ could potentially be increased by recruiting motor units consisting of more powerful fibers. Among bird species, the percentage of larger-diameter, more-glycolytic fibers in the pectoralis scales positively with increasing body mass in woodpeckers (Picidae) but not in doves (Columbidae; Tobalske, 1996; Bosdyk and Tobalske, 1998), so this explanation may be appropriate for some groups of birds but not for others. Other factors that may shape the maximum power available from a cyclically contracting muscle include the proportion of the cycle time spent shortening and the timing of muscle activation and deactivation (Askew and Marsh, 1997, 1998).

We undertook the present study to test whether the scaling of maximal take-off ability was related to *in vivo* muscle contractile properties (ε and σ) and wing kinematics in birds. To help control for variation in morphology, flight ecology and phylogeny that could otherwise contribute to variation about general scaling trends among birds, we selected four species within a single family of birds, the Phasianidae: northern bobwhite (*Colinus virginianus* L.; hereafter, quail), chukar (*Alectoris chukar* Gray), ring-necked pheasant (*Phasianus colchicus* L.; hereafter, pheasant) and wild turkey (*Meleagris gallopavo* L.; hereafter, turkey). In the wild, these species take to the wing almost exclusively to escape from predators (Fig. 1). Their wings are reportedly better-suited for rapid take-off than the wings of some other species in the Phasianidae (Drovetski, 1996), and the pectoralis of all four species is pinkish white in appearance. This appearance reflects a relatively low myoglobin content and a relatively high percentage of fast-glycolytic fibers (Kiessling, 1977; Rosser and George, 1986), characteristics well-suited for burst, but not sustainable, power output. In summary, the species we selected probably represent an extreme design for maximal take-off performance among birds.

Materials and methods

Birds and experimental design

Birds were obtained from commercial suppliers. Experiments were conducted in three locations. All experiments involving quail, chukar and pheasant took place at the University of Montana, Missoula, MT, USA (altitude 970 m above sea level, 46.9° latitude). For this location, gravitational acceleration ($\boldsymbol{g}$) was 9.805 m s^{-2} and average air density (ρ) was 1.115 kg m^{-3} (Lide, 1998). Two turkeys, used in sonomicrometry and electromyography experiments, were studied at the Concord Field Station, Harvard University,

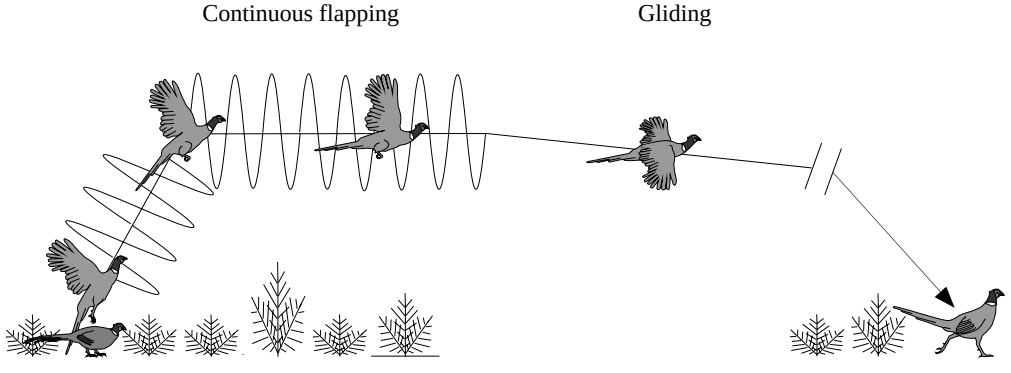

Fig. 1. The flight style of bird species in the Phasianidae. The drawings represent a ring-necked pheasant (*Phasianus colchicus*).

Bedford, MA, USA (41 m altitude, 42.5° latitude, g=9.804 m s^{-2}, ρ=1.220 kg m^{-3}). Lastly, three turkeys, used only for the kinematic study, were video-taped (video footage supplied by S. M. Gatesy) at Wake Forest Unversity, Winston-Salem, NC, USA (278 m altitude, 39.5° latitude, g=9.800 m s^{-2}, ρ=1.193 kg m^{-3}) in association with a different study (Gatesy and Dial, 1996).

We considered take-off to include periods of continuously flapping flight starting with the first downstroke one full wingbeat after a bird's feet were completely off the ground and lasting until the bird began a deceleration or descent for landing. The birds studied at the University of Montana and Harvard University were relatively wild and unpredictable; their take-off trajectories varied between vertical and horizontal, depending upon the individual bird and flight. These birds flew 20 m towards a refuge at the end of a hallway; the refuge was constructed using a cardboard box, shrubs and netting. The three turkeys studied at Wake Forest University, which were relatively accustomed to humans, were trained to fly vertically from the ground to a perch either 1.4 or 1.7 m in height.

Morphometric data were collected from the birds immediately after conducting the experiments (see Table 1). Body mass (g) and pectoralis mass (g; left pectoralis only) were measured using a digital balance. Body weight (N) was calcuated as body mass multiplied by gravitational acceleration, which varied slightly among study locations (see above). Fascicle length (mm) in the region of the pectoralis in which sonomicrometry crystals were implanted (longest fascicles in muscle, Fig. 2) was measured using digital calipers.

We obtained external wing measurements using conventional methods (Pennycuick, 1989; Tobalske, 1996). Wing span (cm) and wing area (cm^2, including the projected area of both wings and the body between the wings) were measured with the wings fully extended and with the feathers spread as in mid-downstroke of flapping flight. We verified the mid-downstroke posture from video and film images obtained during flight (see below). In this posture, the emargination on the distal third of each of the primaries was completely separated from adjacent feathers. Wing span was measured along a straight line between the distal tips of the eighth primaries with the bird ventral side up. Wing area was obtained from wing and body tracings. Each wing was stretched over the side of a table, dorsal side up, with the edge of the table abutting the shoulder of the bird (Pennycuick, 1989). The outline of the stretched wing, including all feathers distal to the proximal end of the humerus, was traced onto paper. This outline was video-taped, and the video image was imported to a computer. The wing outline in the digital image was then traced using NIH Image software, and wing area was converted from pixels within the wing outline to cm^2 using a known scale. Both wings from each bird were measured in this way. We used similar methods to measure body area, but the outline of the body was traced with the bird lying ventral side up. The area of the body included in our measure of wing area was defined cranially by the leading edge of the wing and caudally by the trailing edge of the longest secondaries.

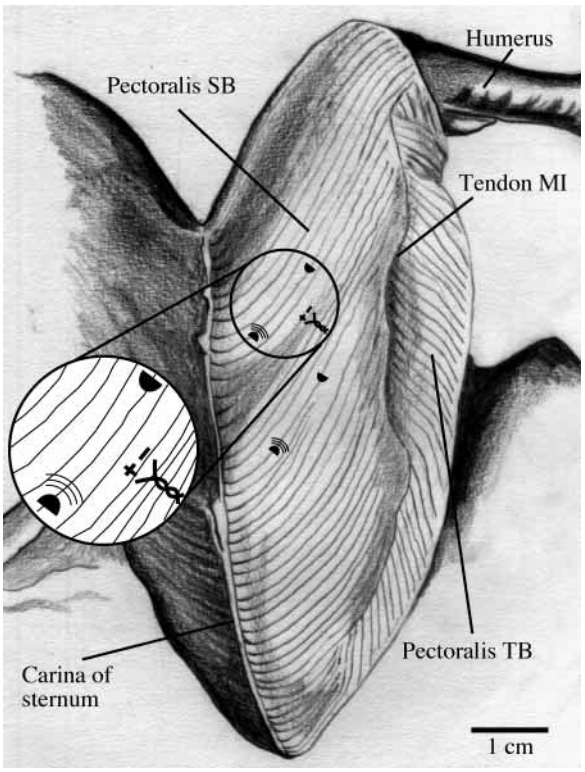

Fig. 2. Ventral view of the pectoralis muscle of the northern bobwhite (*Colinus virginianus*) showing the location where sonomicrometry crystals and bipolar electromyographic electrode were implanted (see expanded region). A second pair of crystals (caudal to the first pair) was implanted in the pectoralis of two wild turkies (*Meleagris gallopavo*) (not to scale). SB, pars sternobrachialis; TB, pars thoracobrachialis; MI, membrana intramuscularis.

Average wing chord (cm) was wing area divided by wingspan. Aspect ratio (dimensionless) was wingspan divided by wing chord. Disc loading (N m^{-2}) and wing loading (N m^{-2}) were computed using body weight divided by disc area and combined wing area, respectively.

Surgical procedures

The left pectoralis muscle was implanted with one pair of sonomicrometry crystals to measure muscle length and one bipolar electromyography (EMG) electrode to measure neuromuscular activity. In addition, in three pheasants, a strain gauge was implanted on the deltopectoral crest of the humerus, and a second pair of sonomicrometry electrodes was implanted in the pectoralis, 2 cm caudal to the first pair of crystals, in two turkeys.

Surgery was performed to implant the transducers and electrodes. Birds were anesthetized using intramuscular injections of ketamine (20 mg kg^{-1}) and xylazine (2 mg kg^{-1}), with additional doses given as needed. The feathers were removed as needed, and minimal incisions were made in the

skin overlying the pectoralis (left side), the thoracic vertebrae and, for strain-gauge implantation, the dorsal, proximal humerus. All recording wires were already soldered to 1–2 miniature connectors (Microtech Inc., GF-6) embedded in an epoxy platform. The platform was sutured to intervertebral ligaments in the dorsal thoracic region and oriented such that the miniature connectors remained externally exposed following surgery.

Sonomicrometry crystals (2 mm disc sonomicrometry crystal, SL2, Triton, Inc.) and an EMG electrode (California Fine Wire Co., twisted pair 100 μm diameter silver wire, 0.5 mm insulation removed at implanted end of wire, tips separated by 1 mm) were passed subcutaneously from the dorsal incision to the incision overlying the pectoralis. The sonomicrometry crystals were implanted in line with the fascicles, facing each other, 1–1.5 cm apart and 0.5 cm deep in the longest fascicles in the pectoralis adjacent to the cranial border of the muscle and less than 3 cm lateral to the keel (Fig. 2). Each sonomicrometry crystal had previously been glued to a stainless-steel wire support that included two small loops (Biewener et al., 1998a,b); these loops were sutured to superficial fascia of the pectoralis.

An EMG electrode was implanted perpendicular to the fascicles, 0.5 cm into the pectoralis and immediately adjacent to a line defined by the two sonomicrometry crystals. The EMG electrode was sutured to superficial fascia, leaving a short loop of wire between the exit point and the fascial suture to allow the electrode tips to move freely.

In an attempt to obtain recordings of bone strain that could be calibrated to estimate force production in the pectoralis muscle, we followed the techniques of Biewener et al. (1992, 1998b), Dial and Biewener (1993) and Dial et al. (1997).

Single-element or rosette strain gauges (FLA-1 and FRA-1, Tokyo Sokki Kenkyujo, Ltd) were implanted in three pheasants on the dorsal surface of the deltopectoral crest (DPC) of the humerus. Access to the DPC was obtained by reflecting the deltoid muscle. Using a periosteal elevator, we removed the periosteum on the dorsal surface of the deltopectoral crest; the bone was then dried using ether applied with a cotton applicator. After drying, a strain gauge was glued to the DPC using cyanoacrylate adhesive. The strain gauge was oriented perpendicular to the long axis of the humerus and immediately adjacent to the anterior edge of the DPC.

Following implantation, all wounds were sutured closed, and the bird was allowed to recover for 24–36 h prior to the start of flight experiments.

Acquisition, correction and calibration of pectoralis data

In vivo muscle data were obtained during take-off flight using 1–2 shielded cables, 20 m in total length, with a mass of 8.4 g per meter of single cable (Cooner Wire, NMUF6). The wires in the cables were soldered to miniature connectors (Microtech Inc., GM-6) connected to an exposed miniature connector on the back of the bird. All signals from the bird were sent to appropriate amplifiers including a Triton 120.2 or Triton System 6 sonomicrometry amplifier, a Grass P5-11 EMG amplifier (gain 1000×, filter 100–3000 Hz bandpass) and a Measurements Group Vishay 2120A strain-gauge signal conditioner/amplifer. The outputs from these amplifiers were sampled at 5 kHz and then stored digitally using either a Keithley 12-bit A/D converter and a Zenith 386X computer or a LabView 16-bit A/D converter and a Power Macintosh 7200 computer. Flights were recorded on film and video for kinematic analyses (see below). Synchronization between the film, video and pectoralis data was obtained by sending electrical pulses generated automatically by the film camera, and manually for the video camera, to separate channels on the A/D converters.

For subsequent analysis, EMG signals remained as recorded in volts, while sonomicrometry and strain-gauge signals were corrected and calibrated. EMG bursts were identified as continuous sequences of spikes with a rectified amplitude at least twice the amplitude of the baseline electrical noise. For each contractile cycle (=wingbeat cycle), we measured the duration of EMG activity in the pectoralis (ms) from onset to offset and also calculated the percentage of the wingbeat cycle during which the muscle was active.

Sonomicrometry signals were corrected to represent the instantaneous fascicle length (mm) in the region of the muscle in which the crystals were implanted (Fig. 2), assuming that length change was uniform throughout the fascicle. The measured distance between the sonomicrometry crystals was increased by 2.7 % to account for the velocity of sound in muscle (1540 m s^{-1}; Goldman and Richards, 1954; Goldman and Heuter, 1956) relative to the value of 1500 m s^{-1} assumed by the Triton 120.2 and System 6. This value was then increased by 0.74 mm to account for the higher velocity of sound through the epoxy lens of the 2 mm electrodes relative to muscle tissue (Biewener et al., 1998a,b). We also corrected for a 5 ms phase delay and a frequency-dependent attenuation in the amplitude of the sonomicrometry signals, both of which were due to the 100 Hz linear phase filter inherent to the Triton 120.2 and System 6 amplifiers. We empirically derived a correction equation for attenuation by injecting a 10 mV square-wave signal into a single channel, varying cycle frequency from 0.1 to 100 Hz, and regressing output attenuation as a function of cycle frequency (least-squares linear regression). This regression yielded a correction factor equal to 0.004(wingbeat frequency)+1.000 (r^2=0.94, P<0.0001). To correct the sonomicrometry voltages for attenuation within a given wingbeat cycle, the absolute difference between an observed instantaneous voltage and the mean voltage in the cycle was increased by multiplying by the correction factor. Lastly, the distance between the crystals during perching, with the wings folded and the pectoralis inactive, was taken to represent crystal separation with the muscle at resting length (L_{rest}), and the sonomicrometry signals were multiplied by the ratio of fascicle length to this between-crystal distance.

Using sonomicrometry data, we obtained several measures of the magnitude and timing of length change (ΔL) in the pectoralis. Pectoralis strain (ε, expressed as a percentage) was calculated as $100(\Delta L/L_{rest})$. Fractional lengthening (%) and

fractional shortening (%) were the proportions of pectoralis strain during which the muscle was longer than or shorter than resting length, respectively. Strain rate ($L\,s^{-1}$, where L is muscle length) was pectoralis strain divided by the time between maximum and minimum length as the muscle shortened during a contractile cycle. We also measured shortening duration (%), the time from maximum to minimum muscle length, relative to total cycle time.

We attempted to calibrate DPC strain in units of *in vivo* pectoralis force as in previous studies of flying birds (Biewener et al., 1992, 1998b; Dial and Biewener 1993; Dial et al., 1997). This method relied upon the assumption that the pectoralis, when producing force, applies a bending moment to the DPC that results in a tensile strain on the dorsal surface of the DPC that is directly proportional to the force produced by the muscle. If this assumption is correct, the *in vivo* force produced by the pectoralis may be estimated using an *in situ* calibration. In such a calibration, direct tension is applied to the DPC by pulling with a known force upon a thread tied around the insertion of the pectoralis insertion to the DPC.

To accomplish a strain-gauge calibration, the bird under study was given an overdose of sodium pentobarbitol ($100\,mg\,kg^{-1}$, intravenously). The intact pectoralis was then connected to a pre-calibrated force transducer using 1 mm diameter braided nylon thread tied around the pectoralis within 2 cm of the muscle's insertion on the DPC. During a series of pull calibrations, the humerus was held extended, as during downstroke, and manually fixed at the shoulder and the elbow. Three pulls were performed at several angular elevations relative to horizontal (0 °, +30 ° and +60 °).

We experienced problems with the strain-gauge technique (see Results) that caused us to abandon our efforts to estimate *in vivo* muscle force. Thus, we report measurements using relative strain on the DPC instead of pectoralis force.

Wing kinematics and whole-body take-off power

Flights were filmed and video-taped using a Red Lakes 16 mm film camera set at either 200 or 300 frames s^{-1} (effective shutter opening of 120 °, exposure times of 1.33 and 1.11 ms $frame^{-1}$, respectively) and a Panasonic Hi-8 video camera (NTSC standard, 60 fields s^{-1}). Film was viewed using a motion-analyzer projector with a frame counter; Hi-8 video was transferred to S-VHS and viewed using a monitor and a Panasonic AG-1960 video recorder with jog-shuttle advance. Flight kinematics were digitized by projecting film or video onto a digitizing pad (Summagraphics Bit Pad Plus) and recording *x*,*y* coordinates using NIH Image software and a Power Macintosh 6500 computer. Subsequent analysis of kinematic data was performed using Excel software (Microsoft, Inc.).

We studied wing motion by digitizing anatomical landmarks (center of head, base of tail, base of wing, wrist and wingtip at the distal end of the eighth primary) in successive frames of film or fields of video. Horizontal and vertical reference lines were also digitized; we corrected all measurements for parallax as needed. In lateral views, the bird flew perpendicular to the line of sight of the camera. For caudal views, we limited our measurements of wing kinematics to portions of the flight path in which the tilt of the body caused the long axis of the bird to be no more than 20 ° out of alignment with the long axis of the camera. Any difference relative to perfect alignment with the camera introduced some error into measurements of wingbeat amplitude (Scholey, 1983), but we were unable to correct for this source of error because we lacked simultaneous caudal and lateral views. Wingbeat amplitude (degrees) was obtained for the wingtip (the radius was shoulder to wingtip) from the maximum caudal-view angle through which the wing traveled during a wingbeat. Wingtip and wrist paths, in both lateral and caudal view, were obtained from digitized points (subsequently connected using Canvas software, Deneba, Inc.) or from manual traces of projected film and video which were then scanned into a Macintosh 6500 computer. We identified the start of downstroke and the start of upstroke using wrist movement rather than movement of the wingtip.

To measure the excess (or marginal) power available for climbing and accelerating during take-off, we defined whole-body take-off power (P_{ta}, W) as:

$$P_{ta} = m[(\boldsymbol{g} + a_v)V_v + a_h V_h]\,,$$

where m is body mass (kg), $\boldsymbol{g}$ is the gravitational acceleration ($m\,s^{-2}$), a_v is the vertical acceleration of the body as indicated by the change in position during flight ($m\,s^{-2}$), a_h is the horizontal acceleration of the body as indicated by the change in position during flight ($m\,s^{-2}$), V_v is the vertical velocity ($m\,s^{-1}$) and V_h is the horizontal velocity ($m\,s^{-1}$). Our measurements of whole-body power were obtained from the beginning of take-off flights, with sampled portions including between 1 and 2.5 m of linear flight. To facilitate comparison of among species, we divided P_{ta} by combined pectoralis mass (kg) to provide a pectoralis mass-specific P_{ta} ($W\,kg^{-1}$).

Statistical analyses

For each variable examined in this study, a mean was computed within each individual bird, and the within-individual means were then averaged to provide a mean ± S.D. within each species. We log-transformed variables and then used reduced-major-axis (RMA) regressions to examine scaling relationships between each dependent variable and body mass (Rayner, 1985). As the species are non-independent, and regression assumes statistical independence among cases, we used independent contrasts to compute the RMA regression formulae, correlation coefficients (r) and P values (d.f.=2) indicating whether the observed correlation was significantly different from zero (Garland et al., 1992; PD Tree Module, version 5.0; Jones et al., 1998). For comparison, and to facilitate interpretation of our results for readers unfamiliar with independent contrasts, we also report scaling exponents for species (non-contrast) data.

To use the independent contrasts method, we employed a hypothesis of the phylogenetic relationships among the four species in our study (Fig. 3). We assumed gradual evolution (Brownian motion) when calculating branch lengths (in time

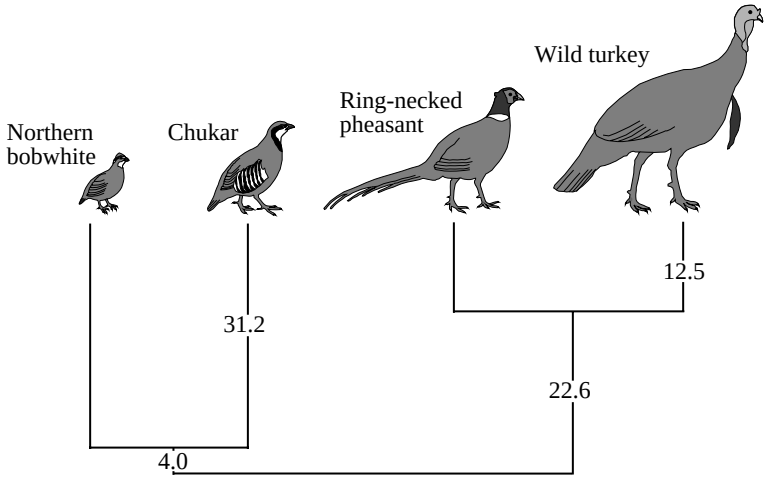

Fig. 3. Hypothesized phylogenetic relationships among four species in the Phasianidae: northern bobwhite (*Colinus virginianus*; quail), chukar (*Alectoris chukar*), ring-necked pheasant (*Phasianus colchicus*) and wild turkey (*Meleagris gallopavo*). Branch lengths are in millions of years.

since divergence) between sister groups. Branch lengths among quail, chukar and pheasant were estimated from Gutiérrez et al. (1983), with a time scale (million years ago) given as 26.3×106*D*, where *D* is Roger's *D*. Time since divergence between pheasant and turkey was estimated from Helm-Bychowski and Wilson (1986). In this case, the range for the origin of turkey was expressed as more than 6–8 million years ago, to which we assigned a value of 7 million years ago. The divergence between turkey and pheasant was described as less than 16–20 million years ago, to which we assigned a value of 18 million years ago. We chose 12.5 million years ago, an average of the two estimated means (7 and 18 million years ago), to reconcile the difference between the two ranges. This brief description provides some insight into the highly approximate nature of the branch lengths indicated in Fig. 3.

We assessed the statistical significance of observed differences in pectoralis strain, fractional lengthening, fractional shortening and strain rate between cranial and caudal fascicles in the turkey pectoralis using paired *t*-tests (N=2, d.f.=1).

Results

Morphometrics

Among the four species in this study, body mass ranged from 199.5±12.6 to 5275.0±1718.3 g. In general, dimensions in the species scaled close to expected values for a model of geometric similarity in which linear dimension scales in proportion to $m^{0.33}$, surface area scales in proportion to $m^{0.67}$ and the mass of body component scales in proportion to $m^{1.0}$ (Table 1). Average wing chord (cm) may represent an exception, for this variable scaled in proportion to $m^{0.42}$ (independent contrasts) or $m^{0.44}$ (species data). Larger birds appeared to have proportionally broader wings, as revealed by the scaling of single wing area (cm^2) in proportion to $m^{0.78}$ or $m^{0.82}$, respectively, and the negative, but non-significant, scaling of aspect ratio.

Table 1. *Morphometric variables (means ± S.D.) and scaling exponents (slopes) for reduced-major-axis regressions describing relationships between log(morphometric variable) and log(body mass)*

	Species						
Variable	Northern bobwhite, N=3	Chukar, N=4	Ring-necked pheasant, N=9	Wild turkey, N=2	Scaling exponent for species data	Scaling exponent for independent contrasts	Correlation coefficient, r
Body mass (g)	199.5±12.6	491.5±66.4	943.4±240.8	5275.0±1718.3	1	1	1
Pectoralis mass (g)	17.3±0.7	35.7±0.7	79.7±22.9	411.9±139.6	0.98	0.97	0.999**
Fascicle length (mm)	39.9±2.7	55.5±3.6	75.6±7.9	126.8±3.9	0.36	0.33	0.992**
Wing span (cm)	34.5±2.2	51.0±2.3	68.1±3.6	119±16.2	0.39	0.36	0.995**
Average wing chord (cm)	7.0±0.5	9.5±0.2	14.7±1.1	28.8±3.8	0.44	0.42	0.994**
Aspect ratio	4.9±0.6	5.4±0.3	4.6±0.3	4.1±0.0	–0.08	–0.08	–0.830
Wing area (cm^2)	242.8±21.8	483.2±21.3	1001.5±110.0	3453.1±919.2	0.82	0.78	0.996**
Disc loading ($N\,m^{-2}$)	21.0±1.4	23.5±1.7	25.1±3.9	45.8±2.7	0.25	0.31	0.967*
Wing loading ($N\,m^{-2}$)	80.8±6.1	99.6±10.1	92.0±17.4	148.6±9.2	0.19	0.23	0.956*

*P<0.05; **P<0.01, d.f.=2.

Correlation coefficients were obtained using independent contrasts.

Wing kinematics

Among species, the wings were always extended maximally during mid-downstroke and a 'tip reversal' (Brown, 1963; Tobalske and Dial, 1996) was exhibited during the upstroke of the initial wingbeats of take-off. From a lateral view, the paths of the wrist and wingtip during these wingbeats gave rise to 'figure-of-eight' loops (Fig. 4A). At mid-upstroke, the distal wing was supinated more than the proximal wing (Fig. 5), the wrists were held relatively close to the midline of the body and superior to the trunk of the bird, and the wingspan between the tips of the eighth primaries was 50 % or more of the wingspan exhibited during the downstroke (Fig. 4B). This wingbeat style is similar to the vortex-ring gait reported for take-off and slow flight in pigeons (*Columba livia*; Brown, 1963; Rayner, 1991b; Tobalske and Dial, 1996).

Subsequent wingbeats during flight were generally similar to the initial wingbeats just described (Figs 4, 5). However, the tip-reversal upstroke was modified so that the wrists and wingtips described elliptical rather than figure-of-eight loops in lateral view, and supination of the distal wing was less prominent than for the wingbeat shown in Fig. 5. The larger species performed more wingbeats before they exhibited a transition to wrist and wingtip paths that were elliptical in lateral view. For example, quail made this transition in four

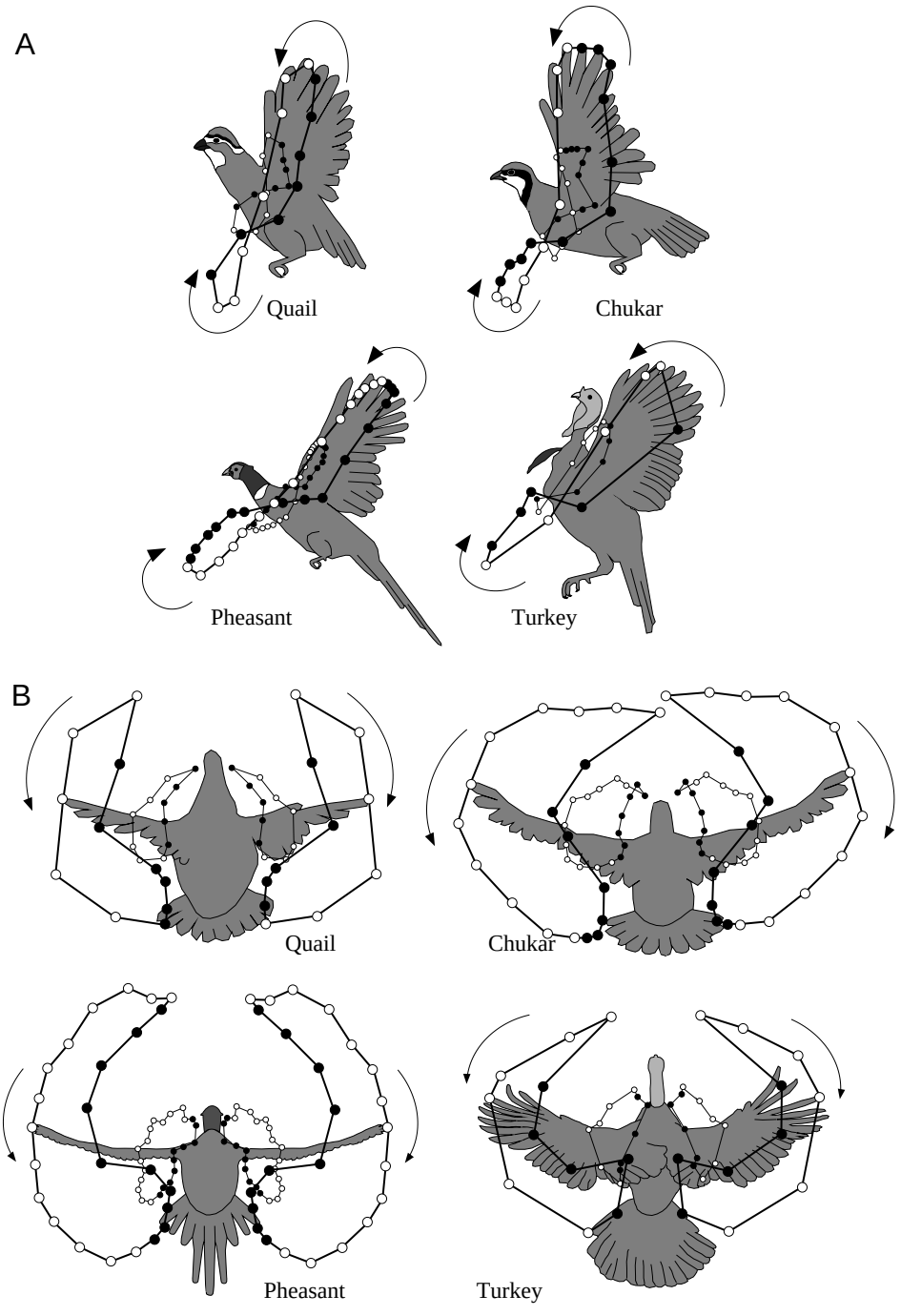

Fig. 4. Lateral and posterior views of take-off flight illustrating the paths of the wingtip and wrist during one wingbeat in four species in the Phasianidae: northern bobwhite (*Colinus virginianus*; quail), chukar (*Alectoris chukar*), ring-necked pheasant (*Phasianus colchicus*) and wild turkey (*Meleagris gallopavo*). (A) Lateral view, with bird silhouettes representing body and wing posture at the beginning of the downstroke, as the wrist begins decreasing in elevation. (B) Posterior view, with bird silhouettes representing body and wing posture at mid-downstroke. Open circles are for the downstroke; filled circles are for the upstroke. Sequences of points are at 300 Hz except for turkey (at 60 Hz) and dorsal-view quail and pheasant at 200 Hz.

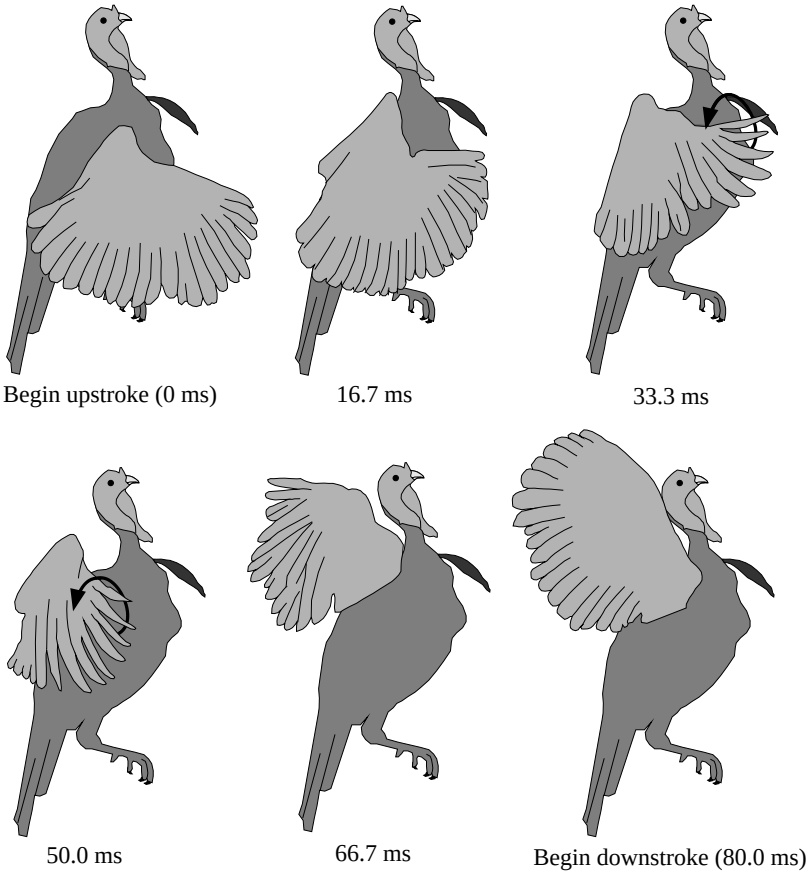

Fig. 5. Successive changes in wing posture during upstroke in the wild turkey (*Meleagris gallopavo*). Arrows illustrate 'wingtip reversal' or supination of the distal wing.

wingbeats or less, whereas the transition in pheasants occurred after 15 wingbeats or more.

Wingbeat frequency decreased as size increased among species, scaling in proportion to $m^{-0.27}$ (independent contrasts) or $m^{-0.31}$ (species data), and wingbeat amplitude (measured in this instance using tip, rather than wrist, excursion) increased among species, scaling in proportion to $m^{0.04}$ (Table 2).

Muscle length changes and the timing of neural activation

Sonomicrometry measurements revealed asymmetrical timing of lengthening *versus* shortening in all four species: the pectoralis shortened for more than 50 % of the duration of a wingbeat cycle (Table 2; Fig. 6). Although the percentage of time the pectoralis spent shortening decreased slightly as body mass increased among species, this relationship was not statistically significant (Table 2).

Pectoralis strain (ε) increased as body mass increased among species from 19.1±4.6 to 35.2±9.3 %, scaling in proportion to $m^{0.23}$ (independent contrasts) or $m^{0.19}$ (species data; Table 2; Fig. 7). The positive scaling of ε with body mass appeared to be due to increases in both fractional lengthening and fractional shortening in the pectoralis, although the correlation between fractional shortening and body mass was not statistically significant.

In contrast to the significant correlation between body mass and ε, strain rate (muscle lengths s^{-1}; $L\,s^{-1}$) did not exhibit a

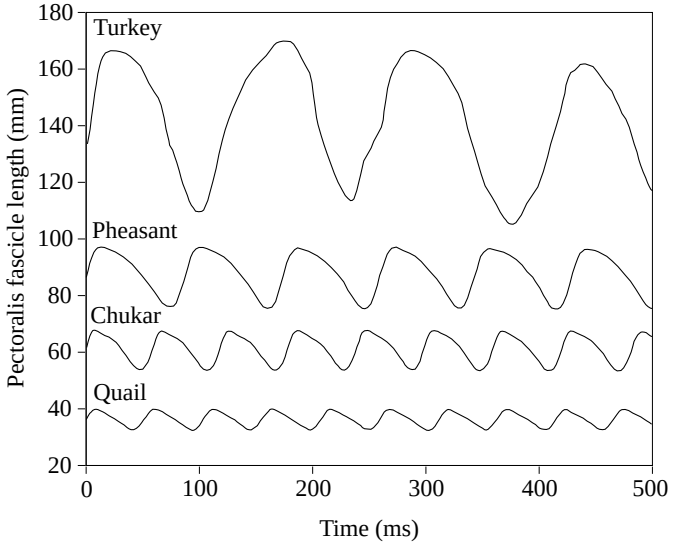

Fig. 6. Sonomicrometry recordings representing length changes in the pectoralis muscle during 500 ms of take-off flight in four species in the Phasianidae: northern bobwhite (*Colinus virginianus*; quail), chukar (*Alectoris chukar*), ring-necked pheasant (*Phasianus colchicus*) and wild turkey (*Meleagris gallopavo*). The 'saw-tooth' shape of sonomicrometry signals appeared consistent with the development of maximal power output according to the *in vitro* study of Askew and Marsh (1997).

Table 2. *Muscle activity, wing kinematics (means + S.D.) and scaling exponents (slopes) for reduced-major-axis regressions describing relationships between log (variable) and log (body mass)*

Variable	Species				Scaling exponent for species data	Scaling exponent for independent contrasts	Correlation coefficient, *r*
	Northern bobwhite, *N*=3	Chukar, *N*=4	Ring-necked pheasant, *N*=9	Wild turkey, *N*=2			
Wingbeat frequency (Hz)	19.9±1.1	16.1±0.5	11.0±1.2	7.6±0.7	–0.31	–0.27	0.975*
Wingbeat amplitude (degrees)[a]	140.3±5.7	151.2±5.1	151.0±6.0	159.9±1.0	0.04	0.04	0.953*
Duration of shortening phase in wingbeat cycle (%)	64.4±2.5	59.1±8.0	56.2±7.0	55.8±1.5	–0.05	–0.04	–0.693
Duration of EMG (ms)	18.5±3.4	22.1±5.9	39.5±4.3	66.8±8.5[c]	0.42	0.37	0.970*
Percentage EMG duration in wingbeat cycle (%)	34.1±2.7	32.0±4.6	42.1±2.4	49.0±11.2[c]	0.14	0.12	0.882
Pectoralis strain, $(\Delta L/L_{rest})100$	19.1±4.6	22.8±2.8	22.2±4.6	35.2±9.3	0.19	0.23	0.968*
Fractional lengthening (%)	10.0±2.1	12.0±3.4	13.7±3.4	20.9±1.3	0.23	0.23	0.998**
Fractional shortening (%)	9.1±2.5	10.8±1.7	8.5±3.2	14.1±7.7	0.16	0.23	0.860
Strain rate ($L\,s^{-1}$)	5.9±1.5	6.3±0.7	4.3±0.8	4.8±0.8	–0.13	–0.11	–0.165
Whole-body take-off power, P_{ta} (W)	5.1±0.6	10.1±2.2	11.7±3.8	48.3±50.8[d]	0.68	0.75	0.991**
Pectoralis mass-specific P_{ta} ($W\,kg^{-1}$)[b]	146.4	141.0	73.5	58.6	–0.33	–0.26	–0.858

[a]Computed using the excursion of the wingtip.
[b]Computed using mean values within species.
[c]*N*=7 wingbeats in one bird.
[d]*N*=3 birds.
*P<0.05; **P<0.01, d.f.=2.
L, muscle length; L_{rest}, resting muscle length; EMG, electromyographic signal.
Correlation coefficients were obtained using independent contrasts.

significant correlation with body mass. Strain rates were lower in pheasant and turkey than in quail and chukar, contributing to an overall RMA regression slope of –0.11 (independent contrasts) or –0.13 (species data, Table 2). However, comparisons between sister taxa (i.e. quail *versus* chukar and pheasant *versus* turkey, Fig. 3) revealed an increase in strain rate with increasing body mass (Table 2).

In the turkey, the only species for which we measured length

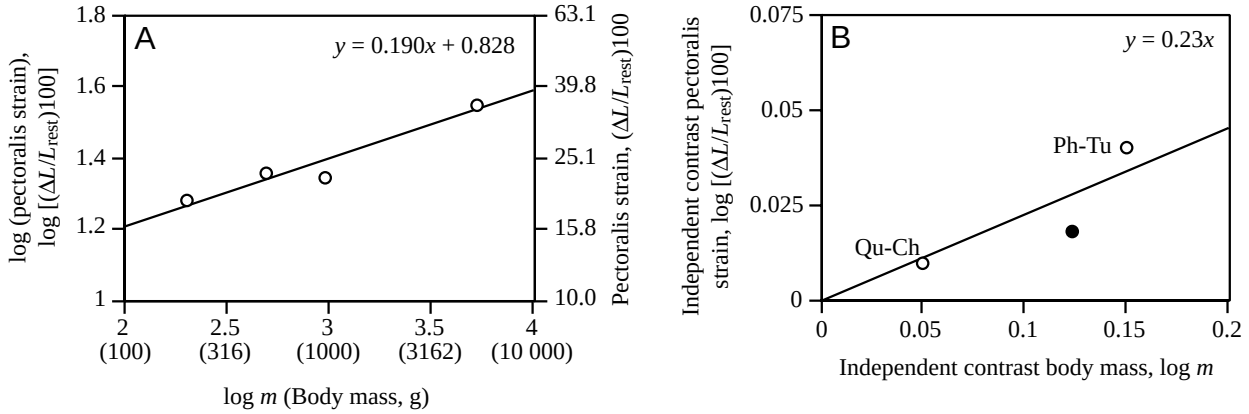

Fig. 7. Reduced-major-axis (RMA) regressions of pectoralis strain in relation to body mass (*m*) in four species in the Phasianidae: northern bobwhite (*Colinus virginianus*; quail), chukar (*Alectoris chukar*), ring-necked pheasant (*Phasianus colchicus*) and wild turkey (*Meleagris gallopavo*). (A) Species data; the line is the RMA regression. (B) RMA regression using standardized independent contrasts. Filled circle, root node; Qu-Ch, northern quail and chukar contrast; Ph-Tu, ring-necked pheasant and wild turkey contrast. L, muscle length; L_{rest}, muscle resting length.

changes in more than one location in the pectoralis, the more caudal fascicles (Fig. 2) exhibited slightly different patterns from the more cranial fascicles included in Table 1. Total strain (36.5±9.6 %), fractional lengthening (23.6+2.5 %) and strain rate (4.8+0.9 $L\,s^{-1}$) were slightly higher, and fractional shortening (12.8+7.2 %) was slightly lower, in the caudal fascicles than in the cranial fascicles. However, the observed differences were not statistically significant (d.f.=1, P>0.05 for each variable).

Consistent with the flexible nature of the avian wing, changes in pectoralis length were more closely synchronized with wrist amplitude than with wingtip amplitude (Fig. 8). In all four species, wrist amplitude was generally at or near maximum when pectoralis length reached a peak value; wingtip amplitude generally reached a maximum after the pectoralis had started to shorten. A similar lag in the timing of distal wing movement relative to proximal wing movement was observed as the pectoralis began lengthening during upstroke.

Electromyographic (EMG) recordings indicated that all the species exhibited a single burst of electrical activity in their pectoralis per wingbeat that featured multiple spikes within each burst (Fig. 9). The duration of EMG activity ranged from 18.5±3.4 to 66.8±8.5 ms and scaled in proportion to $m^{0.37}$ (independent contrasts) or $m^{0.42}$ (species data) (Table 2). The percentage of a wingbeat cycle during which the pectoralis was active showed a slight, non-significant, trend of increasing as body mass increased.

Among species, the onset of pectoralis activity occurred at or near maximum wrist amplitude, and the EMG burst ended during the time interval in which the wrist amplitude was decreasing but before it reached 0° (i.e. before mid-downstroke of the wrist; Fig. 9). Peak amplitude of the wingtip occurred during, or shortly after the end of, the EMG burst from the pectoralis.

Inability to estimate in vivo *muscle force*

The dorsal surface of the deltopectoral crest (DPC) of the humerus proved to be unsuitable for measuring the bending moments produced by the force of contraction in the pectoralis (Fig. 10A). We attempted to obtain the measurements in three pheasants before abandoning this aspect of the study. A representative signal from a single strain gauge wired in a quarter-bridge configuration reveals an inappropriate signal in comparison with the signals obtained from species such as the pigeon (Dial and Biewener, 1993; Fig. 10B). Rather than one rise and fall in tension on the dorsal surface of the DPC during the downstroke that would be consistent with a bending moment as force was produced in the pectoralis, we observed both tensile and compressive strains on the surface of the DPC in the pheasant. This complex pattern of tension and compression was evident in recordings from rosette gauges, which confirmed that it was due to the anatomy of the DPC and pectoralis in the pheasant rather than to a misalignment of a single strain gauge relative to the axis of principal strain. The complex patterns of strain were also apparent during pull

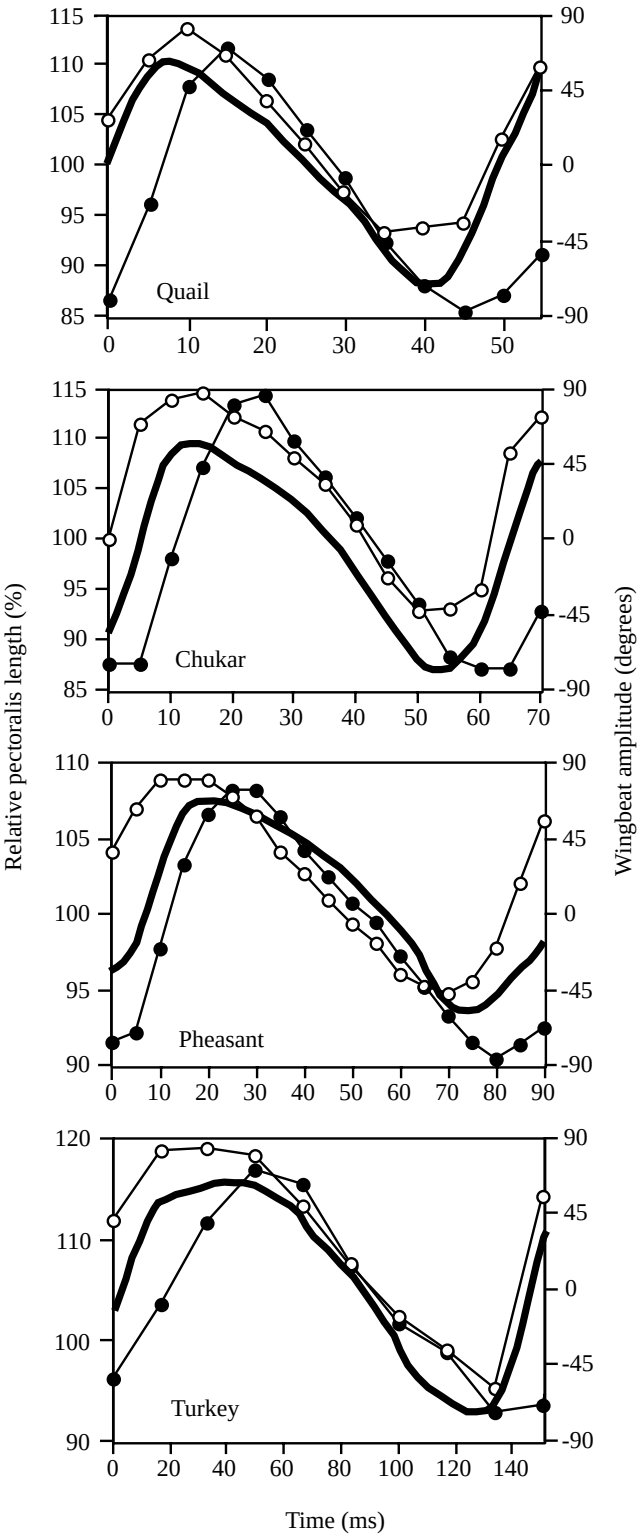

Fig. 8. Pectoralis length (solid line), expressed as a percentage of resting length, in relation to the amplitude of the wing during approximately one wingbeat cycle in four species in the Phasianidae: northern bobwhite (*Colinus virginianus*; quail), chukar (*Alectoris chukar*), ring-necked pheasant (*Phasianus colchicus*) and wild turkey (*Meleagris gallopavo*). Open circles, wrist amplitude; filled circles, wingtip amplitude. Kinematics sampled at 200 Hz except turkey kinematics (sampled at 60 Hz).

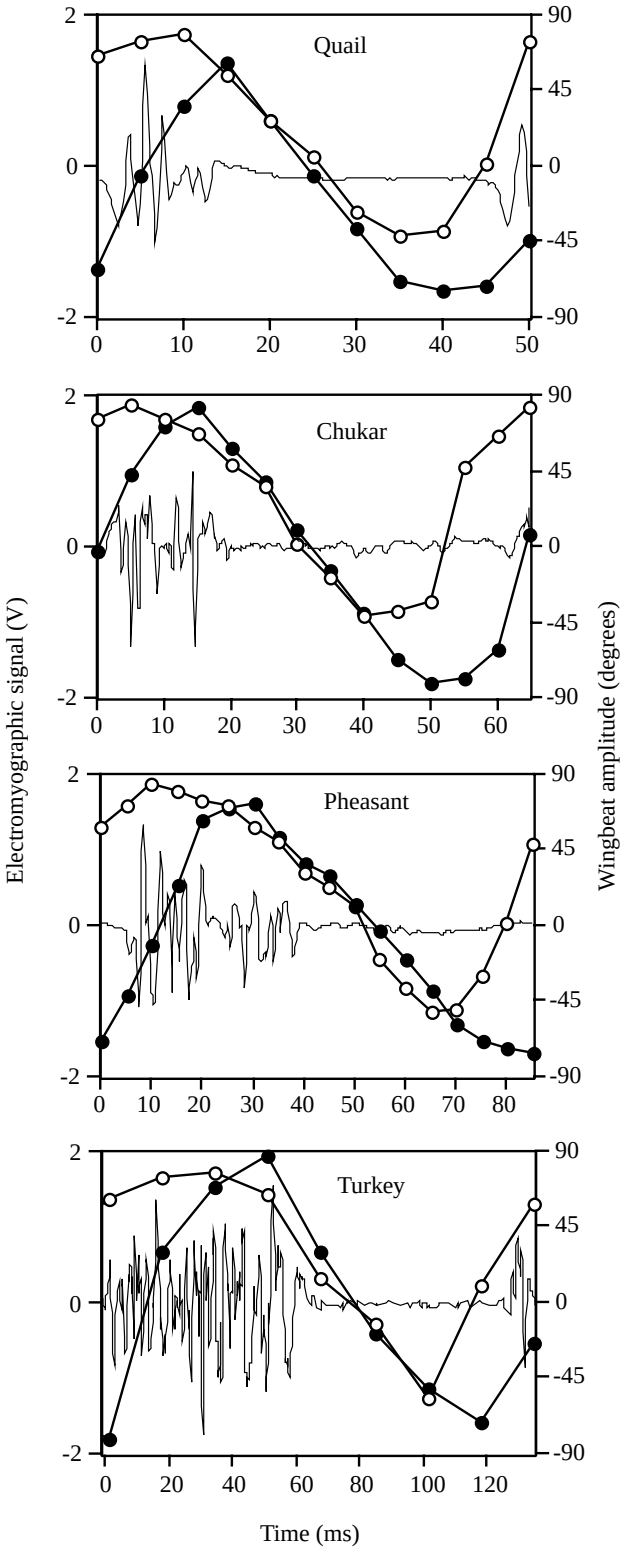

Fig. 9. Electromyographic (EMG) signals from the pectoralis muscle in relation to the amplitude of the wing during approximately one wingbeat cycle in four species in the Phasianidae: northern bobwhite (*Colinus virginianus*; quail), chukar (*Alectoris chukar*), ring-necked pheasant (*Phasianus colchicus*) and wild turkey (*Meleagris gallopavo*). Open circles, wrist amplitude; filled circles, wingtip amplitude. Kinematics sampled at 200 Hz except for the turkey (sampled at 60 Hz).

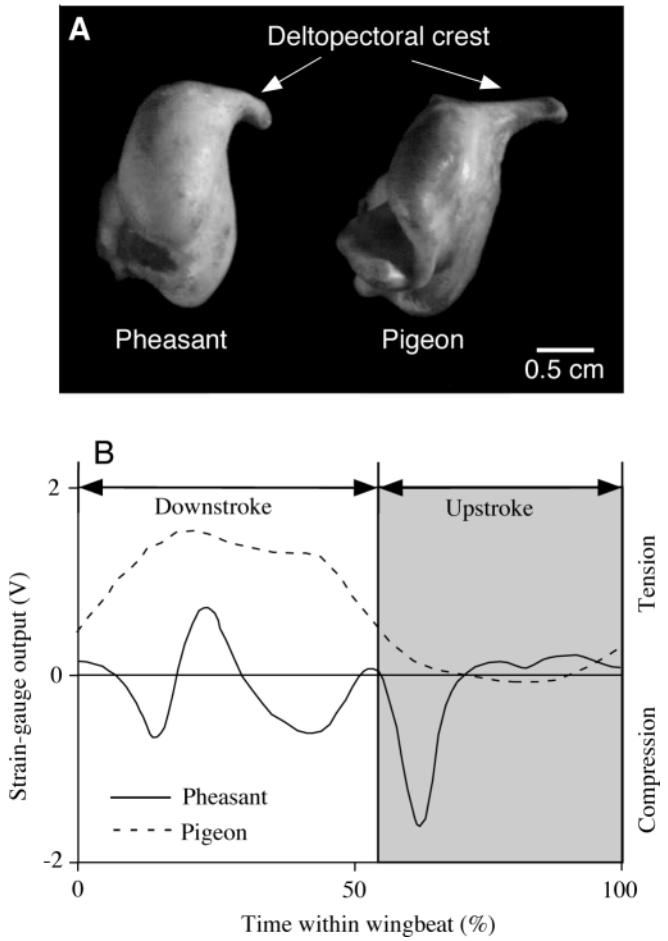

Fig. 10. Anatomy of the deltopectoral crest (DPC) and strain measurements obtained from the DPC during one wingbeat in a ring-necked pheasant (*Phasianus colchicus*) and a pigeon (*Columba livia*). (A) Proximal view of the humerus; arrows indicate the dorsal surface of the DPC onto which the strain gauge was glued. (B) Strain-gauge signals from one wingbeat as a function of percentage of the wingbeat cycle.

calibrations. With the tensile force on the calibration thread held constant, tensile and compressive strains on the dorsal surface of the DPC varied according to the elevation of the humerus above horizontal.

The DPC of the pheasant was proportionally smaller and curved more ventrally than in a pigeon (Fig. 10A). Although it is not evident in Fig. 10A, the intramuscular tendon of the pectoralis inserted closer to the long axis of the humerus in the pheasant than in the pigeon, which suggests that the principal line of pectoralis force acting on the humerus was directed further from the DPC. Apparently, the morphology of the pheasant prevented the DPC from acting as a simple cantilever and exhibiting tension on its dorsal surface when the pectoralis produced tension. The humerus and pectoralis of the quail, chukar and turkey all shared similar anatomy with the pheasant.

We provide the above information as a cautionary note to future researchers considering attaching strain gauges to a

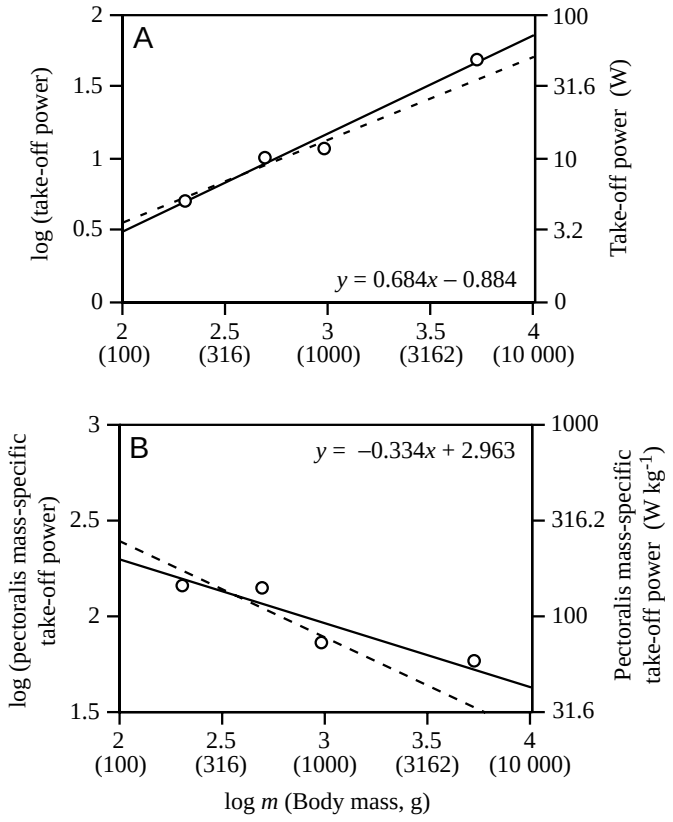

Fig. 11. Reduced-major-axis (RMA) regressions of (A) take-off power (W) and (B) pectoralis mass-specific take-off power ($W\,kg^{-1}$) in four species in the Phasianidae: northern bobwhite (*Colinus virginianus*; quail), chukar (*Alectoris chukar*), ring-necked pheasant (*Phasianus colchicus*) and wild turkey (*Meleagris gallopavo*). Solid lines represent RMA regressions for sample of four species (equations given); dashed lines are RMA regressions with turkeys excluded from the sample (see text for slopes). *m*, body mass.

bird's humerus that the anatomy of the DPC should be structured so that it acts like a simple cantilever for proper strain recording.

Whole-body take-off power

Take-off power (P_{ta}) scaled in proportion to $m^{0.75}$ (independent contrasts) or $m^{0.68}$ (species data). Dividing these values by combined pectoralis mass yielded pectoralis mass-specific P_{ta}, which varied from 146.4 to 58.6 $W\,kg^{-1}$ and scaled in proportion to $m^{-0.26}$ (independent contrasts) or $m^{-0.33}$ (species data). The standard deviation for P_{ta} in the turkey was unusually large (Table 2); this exceptional variability was the result of having a sample with one turkey that consistently decelerated during take-off flight (mean P_{ta} –9.7 W) and two turkeys that consistently accelerated during take-off (mean P_{ta} 77.3 W).

In addition to this high variability, there was potential for motivational differences among species because the turkeys used for measures of P_{ta} were trained to fly to a perch while the other species were untrained and relatively wild. It therefore appeared worthwhile also to obtain RMA regressions of P_{ta} *versus* body mass with turkeys eliminated from the sample (dashed lines in Fig. 11). Among quail, chukar and pheasant, P_{ta} scaled in proportion to $m^{0.57}$ (r=0.966, P not significant, d.f.=1) and pectoralis mass-specific P_{ta} scaled in proportion to $m^{-0.5}$ (r=0.843, P not significant, d.f.=1).

Discussion

Our results provide new insight into how the pectoralis muscle and wings function during maximal take-off in birds of different sizes. The most novel observation was that pectoralis ε increased with increasing body mass (Table 2; Fig. 7). From the classical studies (Hill, 1950) through to efforts in the present, it has been widely assumed that ε is independent of mass in similarly shaped species engaging in comparable activity; this assumption does not appear to be correct for the species in the Phasianidae.

Take-off power (P_{ta}) scaled in proportion to $m^{0.75}$ and pectoralis mass-specific P_{ta} declined with increasing body mass, roughly in direct proportion to wingbeat frequency (Table 2; Fig. 11). Thus, our data were consistent with other studies of escape performance in small flap-bounding birds (DeJong, 1983), aerial insectivores (Warrick, 1998) and doves (Seveyka, 1999). Furthermore, our results appear to support the hypothesis that maximum mass-specific muscle work is invariant with size among species and that wingbeat frequency defines the scaling of mass-specific power available for acceleration and climbing. If this assertion is correct, positive scaling of pectoralis ε with body size (Table 2; Fig. 11) must have been accompanied by a proportional decrease in pectoralis σ in the species in this study. Unfortunately, our inability to estimate *in vivo* pectoralis σ, because of the anatomy of the humerus in the study species (Fig. 10), precluded a rigorous test of this idea.

Ellington (1991) and Marden (1994) suggested that lift-based mechanisms could potentially explain an adverse scaling of power available *versus* that required for flight. The four species in our study were approximately geometrically similar and used similar wing kinematics (Fig. 4), so it appeared unlikely that lift production per unit muscle power output (flight performance *sensu* Marden, 1994) declined with increasing body mass. A flow-visualization study that documents lift during take-off would further test this hypothesis.

Our measure of P_{ta} represents only the mechanical power in excess of aerodynamic (induced, parasite and profile power) and inertial power required for steady-speed, horizontal flight at the same flight speed (Pennycuick, 1975, 1989; Pennycuick et al., 1989; Norberg, 1990). Thus, our data should not be interpreted to represent the total power output from the paired pectoralis muscles (and pectoralis mass-specific P_{ta} should not be mistaken for total pectoralis mass-specific power). Total mechanical power output from the muscles must have been greater to accomplish flight while climbing and accelerating, but we have insufficient data to make a meaningful quantitative comparison among species.

Employing mathematical theory to model the aerodynamic and inertial power of the species in our study may prove worthwhile for estimating total mechanical power output (e.g. Pennycuick, 1975; Rayner, 1979; Norberg, 1990), but this is beyond the scope of the present study. Models should take into account variables we did not measure including interactions between bound circulation on the flapping wings and circulation in the vortex wake as velocity varies during take-off (Rayner, 1995), the contribution of ground effects for birds with different flight trajectories and wing spans (Rayner, 1991a) and the contribution of the legs to the initial take-off velocity (Earls, 2000).

Significant advances in our understanding of muscle contractile properties during cyclical contractions have come from *in vitro* studies by Askew and Marsh (1997, 1998). Their efforts have shown that the optimal shortening velocity at which power output is maximized in skeletal muscle may be affected by factors in addition to the force–velocity relationship (Askew and Marsh, 1997, 1998), including the proportion of a cycle spent shortening and the rate of activation and deactivation. Our results indicate that there may be effects of body size upon contractile dynamics and the timing of neural activation that may merit exploration in future *in vitro* studies. Although the relationships were not statistically significant, as body mass increased among species, the percentage of time that the pectoralis spent shortening and strain rate both decreased, whereas the percentage of time that the pectoralis was active increased (Table 2). The statistical significance of these scaling trends would potentially increase with a larger sample size of species. Our data come from a narrow range of locomotor effort that we assumed was maximal, so it would also be worthwhile to study how these variables change with a wide range of variation in mechanical power output within a single species.

In general, the timing and magnitude of length changes in the pectoralis of the birds in the Phasianidae was consistent with data from the 650 g silver king pigeon engaged in level flight at 5–6 $m\,s^{-1}$ (Biewener et al., 1998b). In all the species, more than 50 % of the contractile cycle is spent shortening, and fractional lengthening relative to resting length is greater than fractional shortening. Pectoralis ε is 32 % in the pigeon, a value within the range of pectoralis ε observed in the Phasianidae (Table 2). Given the differences in fiber types in the pectoralis of pigeons and phasianid birds (Kiesling, 1977; Rosser and George, 1986), it is interesting to note that strain rates are not dramatically different. Strain rate in the pigeon pectoralis varies from 4.9 to 5.4 $L\,s^{-1}$ (Biewener et al., 1998b); these values are roughly in the middle of the range exhibited by the species in the present study. Muscle ε was greater in the more caudal fascicles in the pectoralis of the turkey and the pigeon than in the cranial fascicles. One difference is apparent between species, however. The caudal fascicles of the pectoralis exhibit a lower strain rate than the cranial fascicles in the pigeon (Biewener et al., 1998b), and the reverse was apparent in the turkey.

Brown (1963) reported the use of a wingtip-reversal upstroke in pheasants, but we are the first to report the common use of this wingbeat style among other species in the Phasianidae. The use of a wingtip-reversal upstroke is generally perceived to be a characteristic of birds with relatively long, pointed wings (Rayner, 1991b; Tobalske and Dial, 1996), so it is intriguing that the species in our study used this wingbeat style. Species in the Phasianidae have relatively broad, short wings (Norberg, 1990), and the species we selected are reported to have relatively broad, short wings within the family (Drovetski, 1996).

The aerodynamic function of the wingtip-reversal upstroke is subject to debate. It is understood to occur during the use of a vortex-ring gait, in which all (or most) of the lift produced during a wingbeat is generated by the downstroke (Rayner, 1991b, 1995). There is some evidence that portions of the upstroke may contribute to forward thrust or upward lift (Aldridge, 1986; Corning and Biewener, 1998; Warrick and Dial, 1998; Seveyka, 1999). In contrast, vortex-visualization studies have revealed that the wing is aerodynamically inactive during tip reversal (Spedding et al., 1984; Spedding, 1986; Rayner, 1991b). Another functional role may be that the backward flick associated with the end of a tip reversal enhances lift production during the downstroke (Norberg, 1990; Rayner, 1995). The use of tip reversal in birds that appear to be maximizing their acceleration during take-off suggests a functional role for the upstroke that is distinct from the flexed-wing upstroke observed during the use of a vortex-ring gait in passerines (Tobalske and Dial, 1996; Tobalske et al., 1999).

We wish to thank Doug Warrick, Jerred Seveyka, Wendy Peacock, Mike Williamson, Matt Bundle and Andrew Biewener for their assistance during experiments and for sharing their perspectives on flight mechanics. We thank the staff at the Concord Field Station, Harvard University, for housing turkeys, Stephen Gatesy for providing video footage of turkey flight and Daniel Léger for creating the illustration of quail pectoralis (Fig. 2). Finally, we thank Claudine Tobalske and Karen Dial for their constant support and for accepting our repeated excuses for returning to the nest well after hours. This project was supported by NSF IBN-9507503 to K.P.D.

References

Aldridge, H. D. J. N. (1986). Kinematics and aerodynamics of the greater horseshoe bat, *Rhinolophus ferrumequinum*, in horizontal flight at various flight speeds. *J. Exp. Biol.* **126**, 479–497.

Askew, G. N. and Marsh, R. L. (1997). The effects of length trajectory on the mechanical power output of mouse skeletal muscles. *J. Exp. Biol.* **200**, 3119–3131.

Askew, G. N. and Marsh, R. L. (1998). Optimal shortening velocity (V/V_{max}) of skeletal muscle during cyclical contractions: length–force effects and velocity-dependent activation and deactivation. *J. Exp. Biol.* **201**, 1527–1540.

Biewener, A. A., Corning, W. R. and Tobalske, B. W. (1998a). *In*

vivo pectoralis muscle force–length behavior during level flight in pigeons (*Columba livia*). *J. Exp. Biol.* **201**, 3293–3307.

Biewener, A. A., Dial, K. P. and Goslow, G. E., Jr (1992). Pectoralis muscle force and power output during flight in the starling. *J. Exp. Biol*. **164**, 1–18.

Biewener, A. A., Koneczynski, D. D. and Baudinette, R. V. (1998b). *In vivo* muscle force–length behavior during steady-speed hopping in tammar wallabies. *J. Exp. Biol.* **201**, 1681–1694.

Bosdyk, A. K. and Tobalske, B. W. (1998). Muscle composition and maximum power for flight in doves and pigeons (Columbiformes). *Am. Zool.* **38**, 126A.

Brown, R. H. J. (1963). The flight of birds. *Biol. Rev*. **38**, 460–489.

Chai, P. and Millard, D. (1997). Flight and size constraints: hovering performance of large hummingbirds under maximal loading. *J. Exp. Biol*. **200**, 2757–2763.

Corning, W. R. and Biewener, A. A. (1998). *In vivo* strains in pigeon flight feather shafts: implications for structural design. *J. Exp. Biol*. **201**, 3057–3065.

DeJong, M. J. (1983). Bounding flight in birds. PhD thesis, University of Wisconsin, Madison, USA.

Dial, K. P. and Biewener, A. A. (1993). Pectoralis muscle force and power output during different modes of flight in pigeons (*Columba livia*). *J. Exp. Biol*. **176**, 31–54.

Dial, K. P., Biewener, A. A., Tobalske, B. W. and Warrick, D. R. (1997). Mechanical power output of bird flight. *Nature* **390**, 67–70.

Drovetski, S. V. (1996). Influence of the trailing-edge notch on flight performance in galliforms. *Auk* **113**, 802–810.

Earls, K. D. (2000). Kinematics and mechanics of ground take-off in the starling *Sturnus vulgaris* and the quail *Coturnix coturnix*. *J. Exp. Biol*. **203**, 725–739.

Ellington, C. P. (1991). Limitations on animal flight performance. *J. Exp. Biol*. **160**, 71–91.

Garland, T., Jr., Harvey, P. H. and Ives, A. R. (1992). Procedures for the analysis of comparative data using phylogenetically independent contrasts. *Syst. Biol*. **41**, 18–32.

Gatesy, S. M. and Dial, K. P. (1996). From frond to fan: *Archaeopteryx* and the evolution of short-tailed birds. *Evolution* **50**, 2037–2048.

Goldman, D. E. and Heuter, T. F. (1956). Tabular data of the velocity and absorption of high frequency sound in mammalian tissues. *J. Acoust. Soc. Am*. **28**, 35–53.

Goldman, D. E. and Richards, J. (1954). Measurements of high-frequency sound velocity in mammalian soft tissue. *J. Acoust. Soc. Am*. **26**, 981–983.

Gutiérrez, R. J., Zink, R. M. and Yang, S. Y. (1983). Genic variation, systematic and biogeographic relationships of some galliform birds. *Auk* **100**, 33–47.

Helm-Bychowski, K. M. and Wilson, A. C. (1986). Rates of nuclear DNA evolution in pheasant-like birds: Evidence from restriction maps. *Proc. Natl. Acad. Sci. USA* **83**, 688–692.

Hill, A. V. (1950). The dimensions of animals and their muscular dynamics. *Sci. Prog*. **38**, 209–230.

Jones, J. A., Midford, P. E. and Garland, T., Jr (1998). *Phenotypic Diversity Analysis Program v 5.0*. Madison: University of Wisconsin.

Kiessling, K.-H. (1997). Muscle structure and function in the goose, quail, pheasant, guinea hen and chicken. *Comp. Biochem. Physiol*. **57**B, 287–292.

Lide, D. R. (1998). *CRC Handbook of Chemistry and Physics*, 79th edition 1998–1999. Boca Raton, FL: CRC Press.

Marden, J. (1994). From damselflies to pterosaurs: how burst and sustainable flight performance scale with size. *Am J. Physiol.* **266**, R1077–R1084.

Norberg, U. M. (1990). *Vertebrate Flight: Mechanics, Physiology, Morphology, Ecology and Evolution*. New York: Springer-Verlag.

Pennycuick, C. J. (1975). Mechanics of flight. In *Avian Biology*, vol. 5 (ed. D. S. Farner and J. R. King), pp. 1–75. London: Academic Press.

Pennycuick, C. J. (1989). *Bird Flight Performance: A Practical Calculation Manual.* New York: Oxford University Press.

Pennycuick, C. J. (1992). *Newton Rules Biology: A Physical Approach to Biological Problems.* New York: Oxford University Press.

Pennycuick, C. J., Fuller, M. R. and Mcallister, L. (1989). Climbing performance of Harris' hawks (*Parabuteo unicinctus*) with added load: implications for muscle mechanics and for radiotracking. *J. Exp. Biol*. **142**, 17–29.

Rayner, J. M. V. (1979). A new approach to animal flight mechanics. *J. Exp. Biol.* **80**, 17–54.

Rayner, J. M. V. (1985). Linear relations in biomechanics: The statistics of scaling functions. *J. Zool., Lond. A* **206**, 415–439.

Rayner, J. M. V. (1991a) On the aerodynamics of animal flight in ground effect. *Phil. Trans. R. Soc. B* **334**, 119–128.

Rayner, J. M. V. (1991b). Wake structure and force generation in avian flapping flight. *Acta XX Congr. Int. Orn*. **II**, 702–715.

Rayner, J. M. V. (1995). Dynamics of the vortex wakes of flying and swimming vertebrates. In *Biological Fluid Dynamics* (C. P. Ellington and T. J. Pedley), pp. 131–155. *Symposia of the Society for Experimental Biology XLIX*. Cambridge: The Company of Biologists Limited.

Rosser, B. W. C. and George, J. C. (1986). The avian pectoralis: histochemical characterization and distribution of muscle fiber types. *Can. J. Zool.* **64**, 1174–1185.

Scholey, K. D. (1983). Developments in vertebrate flight: climbing and gliding of mammals and reptiles and the flapping flight of birds. PhD thesis, University of Bristol.

Seveyka, J. J. (1999). Effects of body size and morphology on the flight behavior and escape flight performance of birds. MS thesis, University of Montana.

Spedding, G. R. (1986). The wake of a jackdaw (*Corvus moedulu*s) in slow flight. *J. Exp. Biol*. **125**, 287–307.

Spedding, G. R., Rayner, J. M. V. and Pennycuick, C. J. (1984). Momentum and energy in the wake of a pigeon (*Columba livia*) in slow flight. *J. Exp. Biol*. **111**, 81–102.

Tobalske, B. W. (1996). Scaling of muscle composition, wing morphology and intermittent flight behavior in woodpeckers. *Auk* **113**, 151–177.

Tobalske, B. W. and Dial, K. P. (1996). Flight kinematics of black-billed magpies and pigeons over a wide range of speeds. *J. Exp. Biol*. **199**, 263–280.

Tobalske, B. W., Peacock, W. L. and Dial, K. P. (1999). Kinematics of flap-bounding flight in the zebra finch over a wide range of speeds. *J. Exp. Biol*. **202**, 1725–1739.

Warrick, D. R. (1998). The turning- and linear-maneuvering performance of birds: the cost of efficiency for coursing insectivores. *Can. J. Zool*. **76**, 1063–1079.

Warrick, D. R. and Dial, K. P. (1998). Kinematic, aerodynamic and anatomical mechanisms in the slow, maneuvering flight of pigeons. *J. Exp. Biol*. **201**, 655–672.